

Distribution Feeder Fault Location Using IED and FCI Information

Yanfeng Gong and Armando Guzmán, *Schweitzer Engineering Laboratories, Inc.*

Abstract—Fault location in distribution feeders is a difficult task. Traditional impedance-based fault location methods assume that all feeder sections have the same impedance characteristics. This assumption introduces errors on feeders having sections with different conductor types and different tower configurations. This paper describes a new impedance-based method that uses the impedances and length of each feeder section and relay event reports to calculate possible fault locations. The method is complemented with faulted circuit indicators with communications abilities to reduce the number of possible fault locations. The paper compares calculation results obtained with the traditional and new methods using field cases and shows the benefit of using the new method.

I. INTRODUCTION

A typical distribution feeder has multiple laterals and sublaterals tapped off the main feeder at different locations and provides power to a large geographical area. Fig. 1 illustrates the structure of a typical distribution feeder in which the solid lines indicate the three-phase sections and the dashed lines indicate sections that are not three-phase.

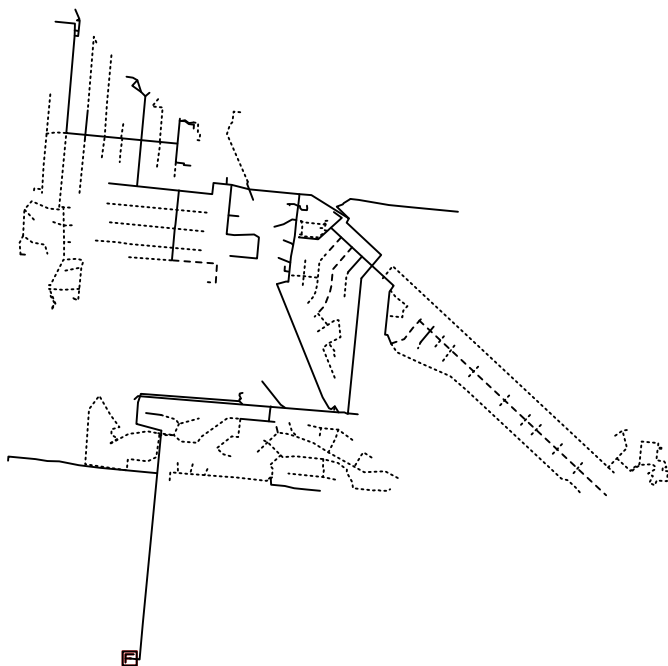


Fig. 1. Typical distribution feeder with hundreds of sections

The ability to locate and clear line faults is critical to minimize the duration and frequency of power outages. Today, many utilities rely on personnel to patrol the feeder to locate faults, which is a time-consuming process. In some difficult cases, line patrol personnel may not be able to locate the faults. The consequences of this fault location approach are increased outage duration and number of outages.

Utilities use the System Average Interruption Duration Index (SAIDI) and the System Average Interruption Frequency Index (SAIFI) as indicators of quality of service (QoS). SAIDI captures the duration (total number of minutes per year) of interruptions experienced by a typical customer. SAIFI captures the frequency (number per year) of interruptions experienced by a typical customer.

The IEEE Working Group on Distribution Reliability reported the SAIDI and SAIFI trends in the United States and Canada; Fig. 2 shows the results from 2004 to 2009 [1]. The challenge for these utilities is to continue the reduction trend of these numbers and improve QoS.

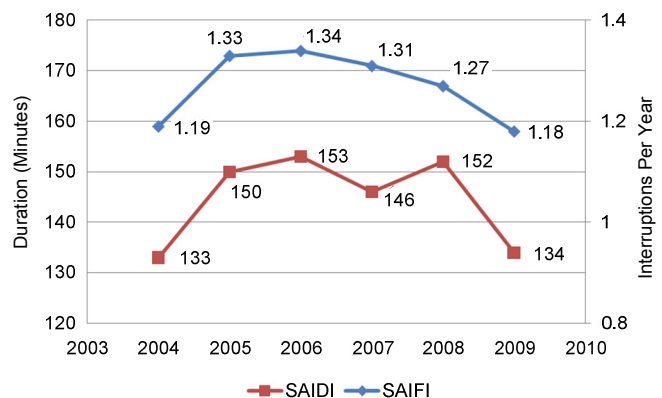


Fig. 2. SAIDI and SAIFI trends in the United States and Canada

One approach to reduce the QoS indicators is to use the fault location information reported by digital relays protecting the feeder at the substation to speed up the fault location process. However, most of the fault location algorithms implemented in digital relays today are designed for homogeneous three-phase lines that have a constant X/R ratio and are not designed for power lines with tapped branches.

Distribution feeders are composed of line sections with different conductor types and tower configurations. Therefore, the line parameters for distribution feeders are rarely homogeneous. Fig. 3 and Fig. 4 show the positive-sequence and zero-sequence line impedances of an actual urban distribution feeder main branch. The result of using a constant X/R ratio is that the reported fault location is different than the actual fault location.

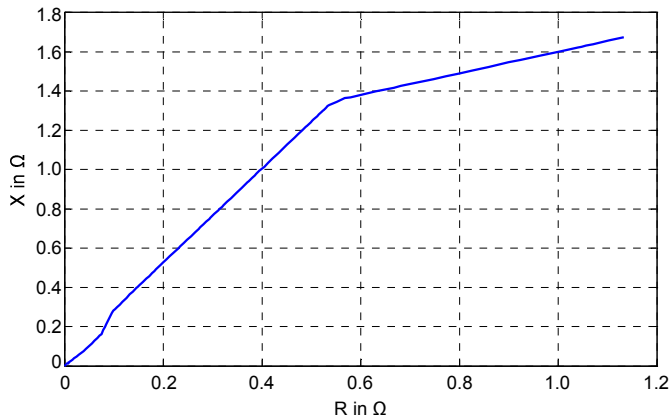


Fig. 3. Distribution feeder positive-sequence impedance is nonhomogeneous

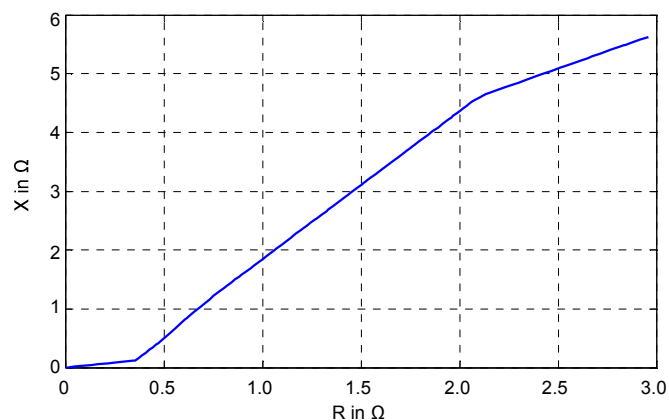


Fig. 4. Distribution feeder zero-sequence impedance is nonhomogeneous

For distribution fault location, some utilities use nomographs to compensate for errors because of the difference between the actual fault location and the fault location calculation of the feeder relay [2] [3] [4]. Creating nomographs is a cumbersome and time-consuming task for the utility. Furthermore, one nomograph is needed for each feeder topology.

Other utilities use the short-circuit analysis results of their distribution feeder and the measured fault current to identify possible fault locations within the feeder [5]. This method can be part of the distribution management system. This approach provides good results so long as the fault resistance is negligible and the short-circuit analysis uses the actual system voltage during the fault.

This paper proposes a fault location method that uses current and voltage measurements recorded by digital relays during fault conditions and accommodates the nonhomogeneous characteristics of distribution. References [6] and [7] proposed similar approaches that use digital fault

recorder information to calculate the apparent reactance to determine the fault location. The method presented in this paper uses these measurements to determine the fault type and calculate the total reactance from the device location to the fault location. Then the method uses the topology information of the feeder to identify the possible fault locations.

For three-phase and phase-to-phase-to-ground faults, the proposed method uses the apparent reactance. For phase-to-phase and phase-to-ground faults, this method uses a reactance calculation based on negative-sequence current to minimize fault location errors due to mutual coupling and balanced loads.

If there is any intelligent electronic device (IED) with current and voltage recording capability installed along the feeder, such as a digital relay or recloser control, this method uses the recorded fault current and voltage measurements from the device that is closest to the fault to improve fault location accuracy. Otherwise, this method uses the event record captured by the digital relay at the substation.

Fig. 5 illustrates a distribution feeder with a recloser control installed in one of the sections of the feeder. For a fault located after the recloser control, this method uses the event report captured by the recloser control. The method then calculates the possible fault locations based on the captured event report and the detailed feeder model. If faulted circuit indicators (FCIs) are available, the method narrows down the possible fault locations depending on the status of the FCIs and reports the estimated fault locations.

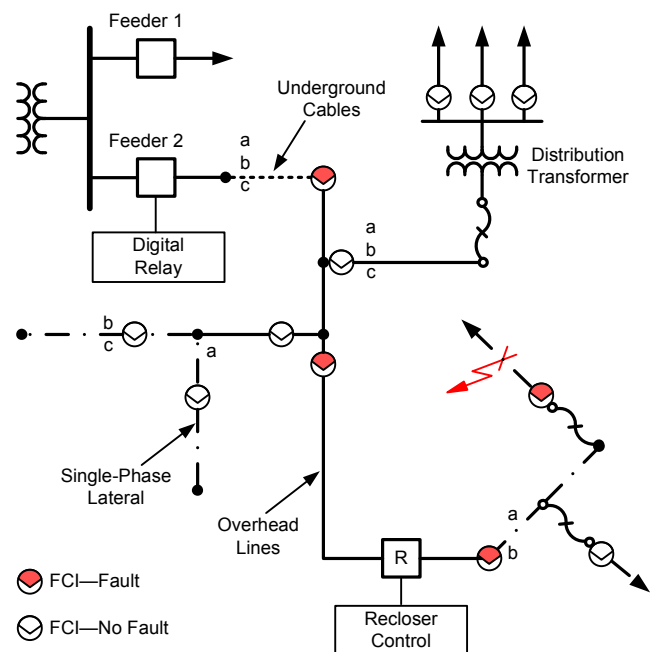


Fig. 5. Distribution feeder with a relay, recloser control, and FCIs

The proposed method is part of an automated system that provides fault information to maintenance and operations personnel within seconds of the occurrence of a fault. With this information, maintenance personnel repair the faulted lines fast, minimizing outage duration and the number of interruptions.

This paper describes the proposed fault location method and shows its performance using two field cases. The first case corresponds to a phase-to-phase fault, and the second case corresponds to a single-phase-to-ground fault. In both cases, the error with respect to the actual fault location is in tens of feet.

II. FAULT LOCATION METHOD

Fig. 6 shows the fault location method that combines reactance calculations using voltage and current measurements with FCI information to determine possible fault locations.

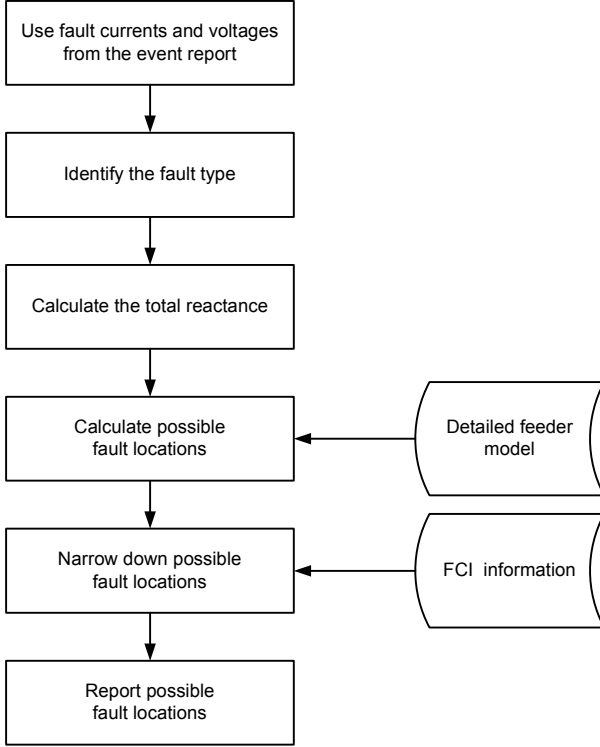


Fig. 6. The fault location method combines reactance calculations with FCI information

The proposed method uses current and voltage measurements acquired during a fault by the relay or recloser control. This information is used to determine the fault type (using the method described in [8]) and calculate the total reactance from the device location to the fault location. The method then calculates the possible fault locations based on the captured event report and the detailed feeder model. Finally, it narrows down the possible fault locations depending on the status of the FCIs (if FCIs are available) and reports the possible fault locations.

A. Total Reactance Calculation

A typical distribution feeder has many line sections with different line impedances. Additionally, there are multiple laterals tapped off the main feeder at different locations. The proposed method calculates only the total reactance from the measuring device to the fault location. All unfaulted laterals are modeled as open circuits during the calculation.

1) Single-Phase-to-Ground Fault

Fig. 7 shows the sequence diagram for a single-phase-to-ground fault with fault resistance R_f on a radial system.

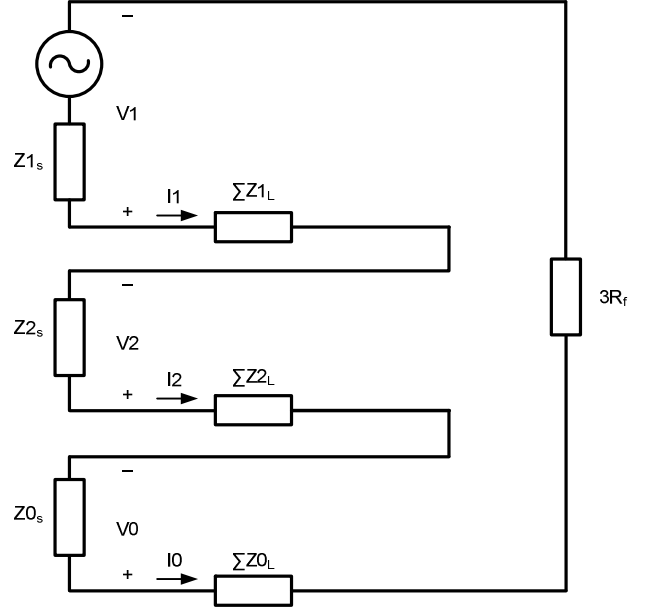


Fig. 7. Sequence diagram for a single-phase-to-ground fault on a radial system

In Fig. 7, V_1 , V_2 , V_0 , I_1 , I_2 , and I_0 are the sequence voltages and sequence currents measured by a digital relay. ΣZ_{1L} , ΣZ_{2L} , and ΣZ_{0L} are the lumped sequence impedances from the relay to the fault. The negative-sequence impedance of each section is the same as the positive-sequence impedance. Based on Fig. 7, we can get (1), where k is the number of line sections between the relay and the fault.

$$\begin{aligned} V_{\text{phase}} &= V_1 + V_2 + V_0 \\ &= \sum_{i=1}^k Z_{1i} \cdot I_1 + \sum_{i=1}^k Z_{2i} \cdot I_2 + \sum_{i=1}^k Z_{0i} \cdot I_0 + 3R_f \cdot I_2 \end{aligned} \quad (1)$$

For a single-phase-to-ground fault, $I_1 = I_2 = I_0$. We can rearrange (1) into (2), where the impedances Z_{1i} , Z_{2i} , and Z_{0i} are separated in their resistance R and reactance X parts.

$$\begin{aligned} V_{\text{phase}} &= \left[\sum_{i=1}^k (R_{1i} + R_{2i} - R_{0i}) + 3R_f \right] \cdot I_2 \\ &\quad + j \cdot \sum_{i=1}^k (X_{1i} + X_{2i} + X_{0i}) \cdot I_2 \end{aligned} \quad (2)$$

Multiplying both sides of (2) by the conjugate of I_2 , rearranging it, and taking the imaginary part only, we calculate the total reactance between the measurement point and the fault, as defined by (3).

$$X_{012_{\text{total}}} = \sum_{i=1}^k (X_{1i} + X_{2i} + X_{0i}) = \frac{\text{Im}(V_{\text{phase}} \cdot I_2^*)}{|I_2|^2} \quad (3)$$

2) Phase-to-Phase Fault

Fig. 8 shows the sequence diagram for a phase-to-phase fault. R_f is the fault resistance between the faulted phases. From Fig. 8, we can get (4).

$$V1 - \left(\sum_{i=1}^k Z1_i + \frac{R_f}{2} \right) \cdot I1 = V2 - \left(\sum_{i=1}^k Z2_i + \frac{R_f}{2} \right) \cdot I2 \quad (4)$$

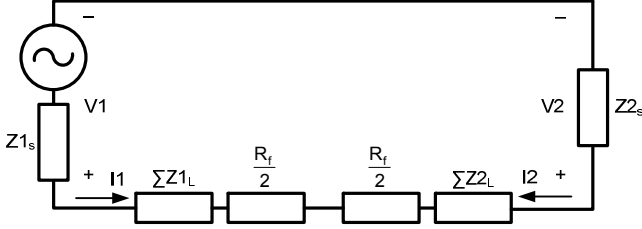


Fig. 8. Sequence diagram for a phase-to-phase fault on a radial system

Because $\sum Z1_L = \sum Z2_L$ and $I1 = -I2$, we can rearrange (4) to get (5). If we take the imaginary parts of both sides of (5), we obtain the calculated total reactance between the measurement point and the fault, as shown in (6).

$$\sum_{i=1}^k Z1_i + \frac{R_f}{2} = \frac{V1 - V2}{I1 - I2} \quad (5)$$

$$X1_{total} = \sum_{i=1}^k X1_i = \text{Im} \left(\frac{V2 - V1}{2 \cdot I2} \right) \quad (6)$$

3) Phase-to-Phase-to-Ground Fault

Fig. 9 shows the sequence diagram for a phase-to-phase-to-ground fault. In this case, the fault resistances R_f and R_g are according to Fig. 10. We use (8) that we obtain from (7) to calculate the total reactance for phase-to-phase-to-ground faults based on the circuit in Fig. 9.

$$\sum_{i=1}^k Z1_i + R_f = \frac{V1 - V2}{I1 - I2} \quad (7)$$

$$X1_{total} = \sum_{i=1}^k X1_i = \text{Im} \left(\frac{V1 - V2}{I1 - I2} \right) \quad (8)$$

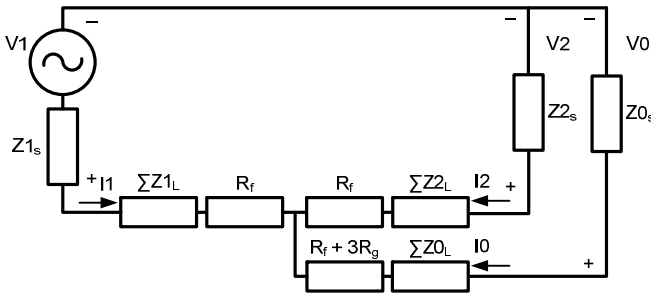


Fig. 9. Sequence diagram for a phase-to-phase-to-ground fault on a radial system

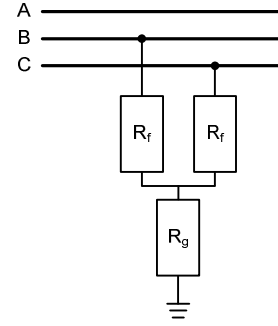


Fig. 10. Fault resistances for a Phase-B-to-Phase-C fault

4) Three-Phase Fault

Fig. 11 shows the sequence diagram for a three-phase fault. From Fig. 11, we can get (9). Rearranging (9) and taking the imaginary parts of both sides of the equation, we can calculate the total reactance for three-phase faults using (10).

$$V1 = \left(\sum_{i=1}^k Z1_i + R_f \right) \cdot I1 \quad (9)$$

$$X1_{total} = \sum_{i=1}^k X1_i = \text{Im} \left(\frac{V1}{I1} \right) \quad (10)$$

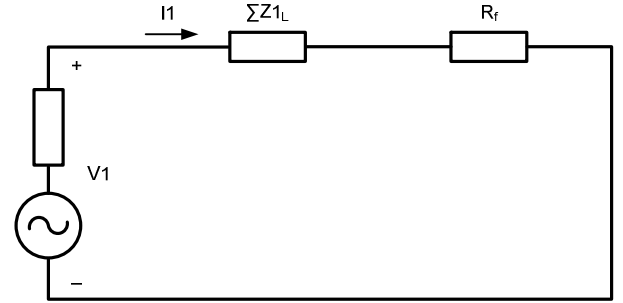


Fig. 11. Sequence diagram for a three-phase fault on a radial system

B. Calculate Fault Locations and Determine Faulted Line Sections

Utilities often model distribution feeders with multiple connected line sections. There are usually some variations in the line section models depending on the distribution analysis software package that they use. However, line sections have some common characteristics as Table I illustrates, although the name of each characteristic may vary.

Each line section has an identification (Section ID). The “From Node ID” and “To Node ID” labels define the connectivity of the line sections. $R1$ and $X1$ are the positive-sequence resistance and reactance for the corresponding line section. $R0$ and $X0$ are the zero-sequence resistance and reactance for the corresponding line section.

TABLE I
TYPICAL LINE SECTION MODEL

Section ID	From Node ID	To Node ID	Phase	Length (ft)	R1 (Ω)	X1 (Ω)	R0 (Ω)	X0 (Ω)
Fd01	Fd0001	Fd0002	ABC	506	0.0662	0.755	0.2497	2.0687
Fd02	Fd0002	Fd0003	ABC	424	0.0452	0.558	0.2140	1.2560

TABLE II
EXAMPLE OF ACCUMULATED LINE REACTANCE CALCULATION

Line Section	Accumulated X1 ($X1_{acc}$)	Accumulated X012 ($X012_{acc}$)	Accumulated Distance (L_{acc})
S1	$X1_{s1}$	$2 \cdot X1_{s1} + X0_{s1}$	L_{s1}
S2	$X1_{s1} + X1_{s2}$	$2 \cdot (X1_{s1} + X1_{s2}) + (X0_{s1} + X0_{s2})$	$L_{s1} + L_{s2}$
S3	$X1_{s1} + X1_{s2} + X1_{s3}$	$2 \cdot (X1_{s1} + X1_{s2} + X1_{s3}) + (X0_{s1} + X0_{s2} + X0_{s3})$	$L_{s1} + L_{s2} + L_{s3}$
S4	$X1_{s1} + X1_{s4}$	$2 \cdot (X1_{s1} + X1_{s4}) + (X0_{s1} + X0_{s4})$	$L_{s1} + L_{s4}$

With the line section information listed in Table I, we can calculate the accumulated reactance (X_{acc}) and the accumulated distance of each line section (L_{acc}). The accumulated reactance of a line section is defined as the sum of the reactance of this line section and the reactances of all other line sections that connect this line section to the device measurement point. The accumulated distance of each line section is the total distance between the device measurement point and the end of the corresponding line section.

We calculate two accumulated reactances, $X012_{acc}$ and $X1_{acc}$, per section. The accumulated reactance values of each line section are defined in Table II for the feeder model shown in Fig. 12. In Fig. 12, $X1_{sk}$, $X0_{sk}$, and L_{sk} are the respective positive-sequence reactance, negative-sequence reactance, and length of line section k .

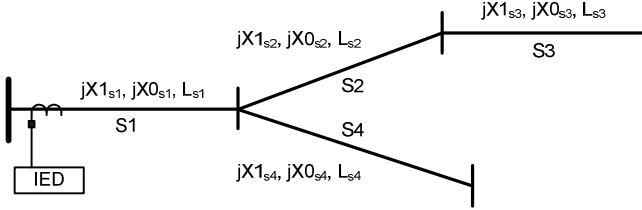


Fig. 12. Simple feeder model for defining the accumulated reactances and distance

The accumulated line reactances and the accumulated distance of each line section can be precalculated if the feeder topology does not change during power system operation. Otherwise, the algorithm calculates these values using the latest topology data obtained in real time.

The general procedure for locating possible faulted line sections and calculating fault locations is as follows:

- Identify the fault type.
- Calculate the total reactance, X_{total_calc} , using (3), (6), (8), or (10) according to the type of fault.
- Search for all line sections that meet the following three conditions:
 - The phase of the line section contains the identified faulted phase.
 - The corresponding accumulated reactance is greater than the calculated total reactance, $X_{acc} \geq X_{total_calc}$.
 - The calculated total reactance is greater than the accumulated line reactance minus the reactance of the present line section, $X_{total_calc} > X_{acc} - X_s$.

- Calculate the fault distance from the measurement point to each faulted line section using (11), where $L_{acc_{sk}}$ and $X_{acc_{sk}}$ are the accumulated distance and accumulated reactance of line section k that was identified by the previous step. X_{sk} and L_{sk} are the reactance and length of line section k .

$$\text{Fault Distance}_{sk} = L_{acc_{sk}} - \frac{X_{acc_{sk}} - X_{total_calc}}{X_{sk}} \cdot L_{sk} \quad (11)$$

The output of this procedure is a list of line sections that are possible faulted line sections together with the corresponding distance to the fault for each possible faulted line section.

C. Incorporate FCI Results

Some distribution feeders may have FCIs installed to facilitate the fault location process. FCIs are able to detect the fault condition and provide an indication whether they detect a fault condition or not. For distribution feeders with a power source at only one end, the fault must be after the line section with an attached FCI detecting a fault condition. With communications abilities, FCIs are able to send a signal that indicates a fault condition back to the IED or computer performing the fault location calculations after a fault has occurred. The additional FCI information can be used to exclude line sections that are not possible faulted line sections. Different methods can be implemented to incorporate the FCI results into the fault locating process. Here, we present one of the many possible implementations.

To integrate the FCI status into the fault location algorithm, we can create a list of associated FCIs for each line section. The list of each line section should contain all the FCIs along the path from the measurement point to the present line section. The list of all the FCIs associated with each line section can be predetermined if the feeder topology does not change. Table III lists the associated FCIs of each line section for the feeder model with FCIs installed at Section S2 and Section S5, as Fig. 13 illustrates.

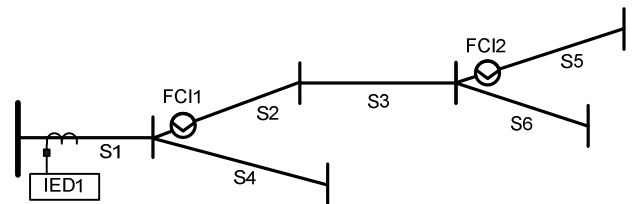


Fig. 13. Simple feeder model with two FCIs and one IED

TABLE III
LINE SECTION WITH ASSOCIATED FCIs

Line Section	Associated FCI List
S1	{}
S2	{FCI1}
S3	{FCI1}
S4	{}
S5	{FCI1, FCI2}
S6	{FCI1}

Depending on FCI deployment, feeders may not have all the FCIs required to discriminate all fault locations. If the fault occurs on line sections that do not have FCIs associated with them, none of the FCIs detect the fault condition. On the other hand, if one or more FCIs detect a fault condition, all the line sections that do not have FCIs associated with them are excluded from the search for the faulted sections.

The algorithm that searches for the faulted line sections requires that all the FCIs associated with the faulted line sections detect the fault condition.

Finally, the line sections with the greatest number of FCIs that detect the fault condition are qualified as possible faulted line sections. Fig. 14 illustrates the procedure for using FCI status to filter out line sections that are not possible faulted line sections. The output of this procedure is the list of all possible faulted line sections.

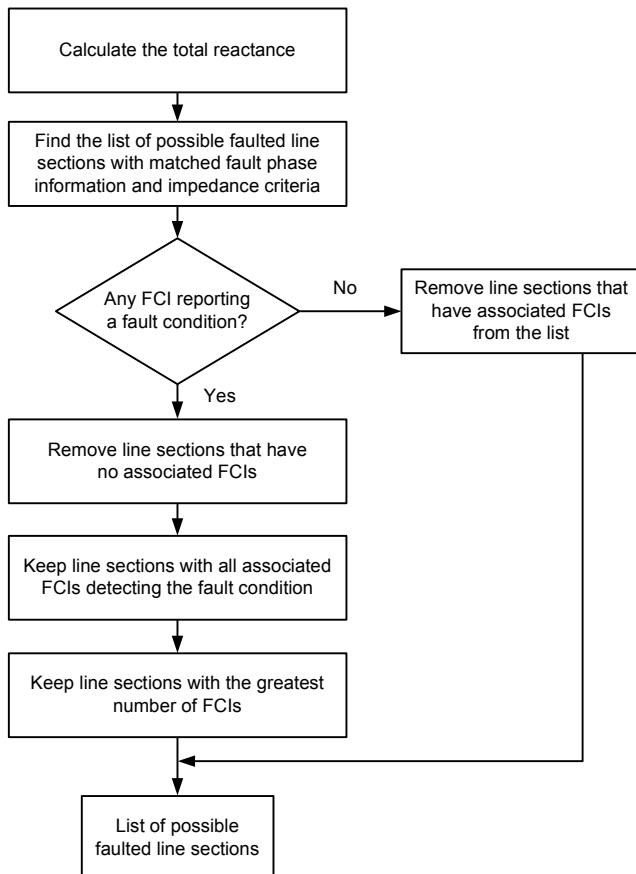


Fig. 14. Procedure for using FCI status to identify possible faulted line sections

D. Feeders With Multiple IEDs

Some distribution feeders may have multiple IEDs, such as recloser controls, in addition to the substation relays. These IEDs can not only detect a fault condition as FCIs do but also record the currents and voltages during the fault. With proper communications infrastructure, there are two ways of incorporating these IEDs into the fault location algorithm.

The first approach treats all the IEDs as FCIs and uses the procedure stated in the previous section to determine the faulted line section. For the simple feeder model shown in Fig. 15, Table IV lists the location information of each IED and Table V shows the association of the FCIs and IEDs to each line section.

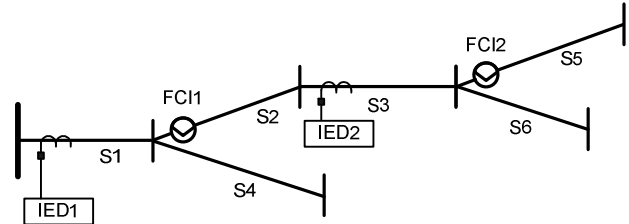


Fig. 15. Feeder model with two FCIs and two IEDs

TABLE IV
IED LOCATION ASSOCIATION

IED Name	Associated Line Section Name
IED1	S1
IED2	S3

TABLE V
LINE SECTIONS WITH ASSOCIATED FCIs AND IEDs

Line Section	Associated FCI and IED List
S1	{IED1}
S2	{IED1, FCI1}
S3	{IED1, FCI1, IED2}
S4	{IED1}
S5	{IED1, FCI1, IED2, FCI2}
S6	{IED1, FCI1, IED2}

The second approach not only treats the IEDs as FCIs but also uses the current and voltage measurements from the IED that is closest to the fault to calculate the total reactance. If the same data table (Table II) is used for locating the faulted line section, the calculated total reactance needs to be offset by adding the accumulated reactance to the point where the IED is installed. If the IED is installed at the beginning of the line section, the offset reactance is equal to the accumulated reactance of the line section subtracted by the reactance of the line section where the IED is installed. If the IED is installed at the end of the line section, the offset reactance is simply the accumulated reactance of the installed line section. With the updated total reactance, the same procedure described in the previous sections can be used to locate the faulted line section.

In the second approach, the errors in the reactance parameters of the line sections between the substation relay and the IED do not affect the fault location accuracy. Therefore, the second approach provides better fault location results if the accuracies of the measurements from the substation relay and the additional IEDs are the same.

III. DISTRIBUTION FAULT LOCATION SYSTEM

The distribution fault location system depicted in Fig. 16 includes the following components:

- Feeder relays
- Recloser controls
- Faulted circuit indicators
- Event collection software
- Fault location software

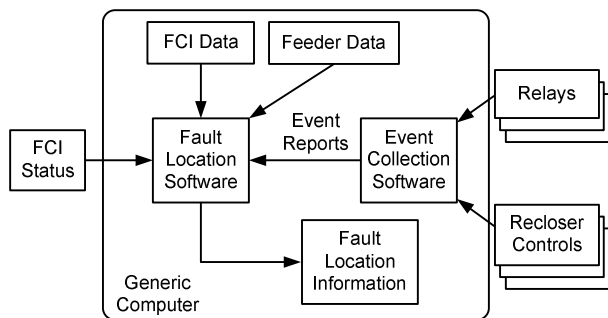


Fig. 16. Distribution fault location system

A. Feeder Relay

The feeder relay is installed at the substation to provide protection against fault conditions. The relay also recloses the breaker to reestablish the power supply to the affected customers after a temporary fault. Additionally, it generates event reports when feeder faults occur. The event reports include the phase voltages and currents measured during the fault.

B. Recloser Control

The recloser control protects several sections of the feeder and closes the recloser to reestablish the power supply after a temporary fault. The control also generates event reports for faults within the protected sections.

C. Faulted Circuit Indicators

The wireless FCIs indicate if the section current exceeds a predefined threshold to discriminate between faults and normal operating conditions.

D. Event Collection Software

The event collection software collects event reports from relays and recloser controls after feeder faults occur. The software can poll the relays and recloser controls to detect new events or retrieve the events as soon as the IEDs notify the software of an event occurrence. Then the software downloads the event reports to a user-defined directory.

E. Fault Location Software

The fault location software uses feeder topology data, feeder data, FCI locations, IED event reports, and FCI status information to identify the possible fault locations. The fault location software provides text and graphical information of the possible fault locations. The result can be sent via email to the proper personnel or published by a web server.

The event collection software and the fault location software run on a generic computer. The fault location software can obtain the status of the FCI from an external real-time database.

IV. FIELD CASE STUDIES

The first case study is a phase-to-phase fault that occurred on a 13 kV distribution feeder. Fig. 17 shows the voltages and currents recorded during the fault by a digital relay. The true fault location reported by line patrol personnel is 11,140 feet from the substation and is at the end of Section Fd00066. The relay-reported fault location is 9,504 feet, with an error of 1,636 feet. The proposed fault location method calculates that the total reactance is 1.27 Ω by using (6). The detailed line model of this feeder has a total of 533 line sections.

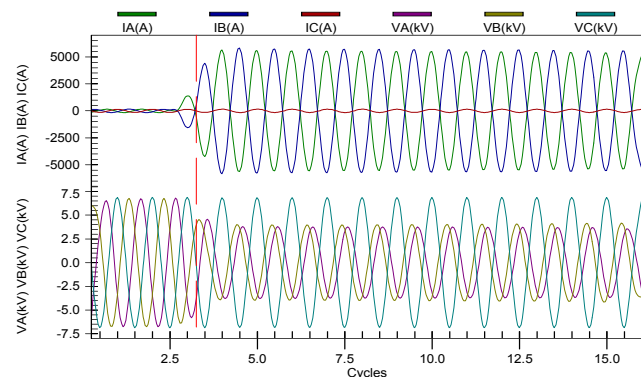


Fig. 17. Recorded fault voltages and currents for a phase-to-phase fault at the end of Section Fd00066

TABLE VI
CASE STUDY 1 FEEDER LINE SECTION DATA

Section ID	From Node ID	To Node ID	Conductor Type	Phase	Length (ft)	R1 (Ω)	X1 (Ω)	R0 (Ω)	X0 (Ω)
Fd00006	Fd00006	Fd00064	750CU	ABC	1077	0.0560	0.0436	0.2040	0.0699
Fd00065	Fd00064	Fd00065	795AAC	ABC	3509	0.0797	0.4060	0.5078	1.5072
Fd00066	Fd00065	Fd00066	336AAC	ABC	6554	0.3451	0.8179	1.1449	2.8827
Fd00067	Fd00066	Fd00067	336AAC	ABC	141	0.0075	0.0178	0.0247	0.0620
Fd00167	Fd00066	Fd00167	336AAC	ABC	93	0.0049	0.0117	0.0163	0.0409

Table VI lists the line sections that are related to this fault. Table VII lists the accumulated impedances and accumulated distance for each section. Because there is no FCI installed on this feeder, the associated FCI list of each line section is omitted from the table.

TABLE VII
CASE STUDY 1 LINE SECTION INFORMATION FOR
FAULT LOCATION CALCULATION

Section ID	Accumulated X1	Accumulated X012	Accumulated Distance
Fd00006	0.04357	0.15704	1077
Fd00065	0.44957	2.47624	4586
Fd00066	1.26747	5.25694	11140
Fd00067	1.28527	5.35454	11281
Fd00167	1.27917	5.32124	11233

The proposed fault location method identifies that the fault is at either Section Fd00067 or Fd00167, with a total distance from the substation of 11,160 feet. The error of using the new method is only 20 feet. If an FCI were installed on either Section Fd00067 or Fd00167, the new method would be able to identify the single fault location.

The second case is a single-phase-to-ground fault on a different 13 kV distribution feeder. Fig. 18 shows the voltages and currents recorded during the fault by a digital relay. The true fault location reported by line patrol personnel is 8,667 feet from the substation at the end of Section Fd00055. The relay-reported fault location is 6,970 feet, with an error of 1,697 feet. The new fault location method calculates that the total reactance (X012) is 4.996 Ω by using (3). The corresponding fault location is 8,691 feet from the substation, with an error of 24 feet. The detailed line model of this feeder has a total of 375 line sections.

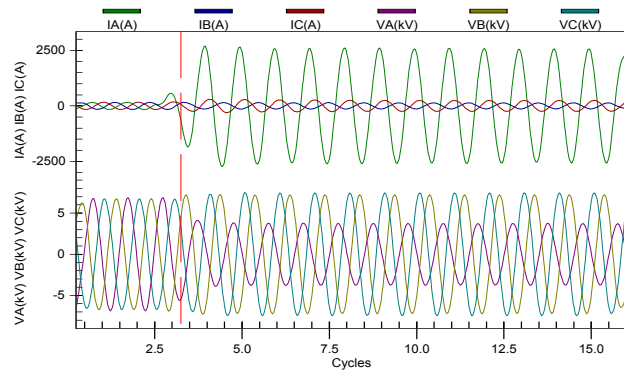


Fig. 18. Recorded fault voltages and currents for a phase-to-ground fault at the end of Section FD00055

TABLE VIII
CASE STUDY 2 FEEDER LINE SECTION DATA

Section ID	From Node ID	To Node ID	Conductor Type	Phase	Length (ft)	R1 (Ω)	X1 (Ω)	R0 (Ω)	X0 (Ω)
Fd00005	Fd00005	Fd00051	750CU	ABC	1872	0.2685	0.0719	0.3542	0.1211
Fd00051	Fd00051	Fd00052	336AAC	ABC	669	0.0352	0.0843	0.1168	0.2942
Fd00052	Fd00052	Fd00053	795AAC	ABC	1006	0.0229	0.1164	0.1457	0.4321
Fd00053	Fd00053	Fd00054	336AAC	ABC	90	0.0047	0.0113	0.0157	0.0396
Fd00054	Fd00054	Fd00055	4/0 CU	ABC	815	0.0429	0.1070	0.1426	0.3936
Fd00055	Fd00055	Fd00056	336AAC	ABC	4215	0.2219	0.5309	0.7362	1.8536

Table VIII lists the line sections that are related to this fault. Table IX lists the accumulated impedances and accumulated distance for each section.

TABLE IX
CASE STUDY 2 LINE SECTION INFORMATION FOR
FAULT LOCATION CALCULATION

Section ID	Accumulated X1	Accumulated X012	Accumulated Distance
Fd00005	0.07187	0.26483	1872
Fd00051	0.15617	0.72763	2541
Fd00052	0.27257	1.39253	3547
Fd00053	0.28387	1.45473	3637
Fd00054	0.39087	2.06233	4452
Fd00055	0.92177	4.97773	8667

These two field cases demonstrate that the reported reactance-based fault location method can provide accurate fault location on distribution feeders. The accurate feeder models developed by the utility company and the light load conditions when the faults occurred contributed to the exceptional accuracy of these two cases.

V. CONCLUSION

This paper presents an automated fault location system for distribution networks. The system uses relays, recloser controls, and FCIs and is suitable for feeders with multiple sections with different impedance characteristics. The fault location algorithm and the automated system have the following characteristics:

- The system uses impedance and length information from each feeder section to accommodate the nonhomogeneity of the feeder.
- The algorithm uses the negative-sequence current and phase voltage to calculate fault location for single-phase-to-ground faults. Using negative-sequence current minimizes errors due to mutual coupling and loads.

- The fault location method calculates reactance to the fault from the IED that is closest to the fault to reduce errors caused by inaccurate line parameters.
- FCIs aid in reducing the number of possible fault locations and minimizing the outage duration.

VI. ACKNOWLEDGMENT

The authors would like to thank Oncor for providing the line parameters and fault event reports of the field cases presented in this paper.

VII. REFERENCES

- [1] Distribution Reliability Working Group, "IEEE Benchmarking 2009 Results," July 2010. Available: <http://grouper.ieee.org/groups/td/dist/sd/doc/2010-07-Benchmarking-Results-2009.pdf>.
- [2] IEEE Guide for Determining Fault Location on AC Transmission and Distribution Lines, IEEE C37.114-2004.
- [3] E. O. Schweitzer, III, "A Review of Impedance-Based Fault Locating Experience," proceedings of the 14th Annual Iowa-Nebraska System Protection Seminar, Omaha, NB, October 1990.
- [4] K. Zimmerman and D. Costello, "Impedance-Based Fault Location Experience," proceedings of the 58th Annual Conference for Protective Relay Engineers, College Station, TX, April 2005.
- [5] M. M. Saha, J. J. Izykowski, and E. Rosolowski, *Fault Location on Power Networks*. Springer-Verlag London Limited, 2010.
- [6] M. M. Saha, F. Provoost, and E. Rosolowski, "Fault Location Method for MV Cable Network," proceedings of the 7th International Conference on Developments in Power System Protection, Amsterdam, Netherlands, April 2001.
- [7] R. Das, "Determining the Locations of Faults in Distribution Systems," PhD thesis, University of Saskatchewan Library, Electronic Theses & Dissertations, 1998. Available: <http://library2.usask.ca/theses/available/etd-10212004-001150/>.
- [8] E. O. Schweitzer, III and J. Roberts, "Distance Relay Element Design," proceedings of the 46th Annual Conference for Protective Relay Engineers, College Station, TX, April 1993.

VIII. BIOGRAPHIES

Yanfeng Gong received his BSEE from Wuhan University, China, in 1998, his MSEE from Michigan Technological University in 2002, and his PhD in electrical engineering from Mississippi State University in 2005. He is currently working as a lead research engineer at Schweitzer Engineering Laboratories, Inc., in Pullman, Washington. He is a member of IEEE and a registered professional engineer in the state of Washington.

Armando Guzmán received his BSEE with honors from Guadalajara Autonomous University (UAG), Mexico. He received a diploma in fiber-optics engineering from Monterrey Institute of Technology and Advanced Studies (ITESM), Mexico, and his MSEE from the University of Idaho, USA. He served as regional supervisor of the Protection Department in the Western Transmission Region of the Federal Electricity Commission (the Mexican electrical utility company) in Guadalajara, Mexico, for 13 years. He lectured at UAG and the University of Idaho in power system protection and power system stability. Since 1993, he has been with Schweitzer Engineering Laboratories, Inc., in Pullman, Washington, where he is a research engineering manager. He holds numerous patents in power system protection and metering. He is a senior member of IEEE.